TECHNICAL REPORT

ISO/TR 11146-3

First edition
2004-02-01

Lasers and laser-related equipment — Test methods for laser beam widths, divergence angles and beam propagation ratios —

Part 3: Intrinsic and geometrical laser beam classification, propagation and details of test methods

Lasers et équipements associés aux lasers — Méthodes d'essai des largeurs du faisceau, des angles de divergence et des facteurs de propagation du faisceau —

Partie 3: Classification intrinsèque et géométrique du faisceau laser, propagation et détails des méthodes d'essai

Reference number
ISO/TR 11146-3:2004(E)

ISO copyright office
Case postale 56 • CH-1211 Geneva 20
Tel. + 41 22 749 01 11
Fax + 41 22 749 09 47
E-mail copyright@iso.org
Web www.iso.org

Published in Switzerland

Contents

Page

Foreword

ISO (the International Organization for Standardization) is a worldwide federation of national standards bodies (ISO member bodies). The work of preparing International Standards is normally carried out through ISO technical committees. Each member body interested in a subject for which a technical committee has been established has the right to be represented on that committee. International organizations, governmental and non-governmental, in liaison with ISO, also take part in the work. ISO collaborates closely with the International Electrotechnical Commission (IEC) on all matters of electrotechnical standardization.

International Standards are drafted in accordance with the rules given in the ISO/IEC Directives, Part 2.

The main task of technical committees is to prepare International Standards. Draft International Standards adopted by the technical committees are circulated to the member bodies for voting. Publication as an International Standard requires approval by at least 75 % of the member bodies casting a vote.

In exceptional circumstances, when a technical committee has collected data of a different kind from that which is normally published as an International Standard ("state of the art", for example), it may decide by a simple majority vote of its participating members to publish a Technical Report. A Technical Report is entirely informative in nature and does not have to be reviewed until the data it provides are considered to be no longer valid or useful.

Attention is drawn to the possibility that some of the elements of this document may be the subject of patent rights. ISO shall not be held responsible for identifying any or all such patent rights.

ISO/TR 11146-3 was prepared by Technical Committee ISO/TC 172, *Optics and photonics*, Subcommittee SC 9, *Electro-optical systems*.

This first edition of ISO/TR 11146-3, together with ISO 11146-1, cancels and replaces ISO 11146:1999, which has been technically revised.

ISO 11146 consists of the following parts, under the general title *Lasers and laser-related equipment — Test methods for laser beam widths, divergence angles and beam propagation ratios*:

— *Part 1: Stigmatic and simple astigmatic beams*

— *Part 2: General astigmatic beams*

— *Part 3: Intrinsic and geometrical laser beam classification, propagation and details of test methods* (Technical Report)

Introduction

The propagation properties of every laser beam can be characterized within the method of second-order moments by ten independent parameters. However, most laser beams of practical interest need less parameters for a complete description due to their higher symmetry. These beams are stigmatic or simple astigmatic, e.g. due to the used resonator design.

The theoretical description of beam characterization and propagation as well as the classification of laser beams based on the second-order moments of the Wigner distribution is given in this part of ISO 11146.

The measurement procedures introduced in ISO 11146-1 and ISO 11146-2 are essentially based on (but not restricted to) the acquisition of power (energy) density distributions by means of matrix detectors, as for example CCD cameras. The accuracy of results based on these data depends strongly on proper data pre-processing, namely background subtraction and offset correction. The details of these procedures are given here.

In some situations accuracy obtainable with matrix detectors might not be satisfying or matrix detectors might simply be unavailable. In such cases, other, indirect methods for the determination of beam diameters or beam width are viable alternatives, as long as comparable results are achieved. Some alternative measurement methods are presented here.

Lasers and laser-related equipment — Test methods for laser beam widths, divergence angles and beam propagation ratios —

Part 3: Intrinsic and geometrical laser beam classification, propagation and details of test methods

1 Scope

This part of ISO 11146 specifies methods for measuring beam widths (diameter), divergence angles and beam propagation ratios of laser beams in support of ISO 11146-1. It provides the theoretical description of laser beam characterization based on the second-order moments of the Wigner distribution, including geometrical and intrinsic beam characterization, and offers important details for proper background subtraction methods recommendable for matrix detectors such as CCD cameras. It also presents alternative methods for the characterization of stigmatic or simple astigmatic beams that are applicable where matrix detectors are unavailable or deliver unsatisfying results.

2 Second-order laser beam characterization

2.1 General

Almost any coherent or partially coherent laser beam can be characterized by a maximum of ten independent parameters, the so-called second-order moments of the Wigner distribution. Laser beams showing some kind of symmetry, stigmatism or simple astigmatism, need even fewer parameters. The knowledge of these parameters allows the prediction of beam properties behind arbitrary aberration-free optical systems.

Here and throughout this document the term “power density distribution $E(x,y,z)$” refers to continuous wave sources. It might be replaced by “energy density distribution $H(x,y,z)$” in the case of pulsed sources. Furthermore, a coordinate system is assumed where the z axis is almost parallel to the direction of beam propagation and the x and y axes are horizontal and vertical, respectively.

2.2 Wigner distribution

The Wigner distribution $h(x,y,\Theta_x,\Theta_y;z)$ is a general and complete description of narrow-band coherent and partially coherent laser beams in a measurement plane. Generally speaking, it gives the amount of beam power of a beam passing the measurement plane at the lateral position (x,y) with a horizontal paraxial angle of Θ_x and a vertical paraxial angle of Θ_y to the z axis, as shown in Figure 1.

NOTE The Wigner distribution is a function of the axial location z, i.e. the Wigner distribution of the same beam is different at different z locations. Hence, quantities derived from the Wigner distribution are in general also functions of z. Throughout this document this z dependence will be dropped. The Wigner distribution then refers to an arbitrarily chosen location z, the measurement plane.

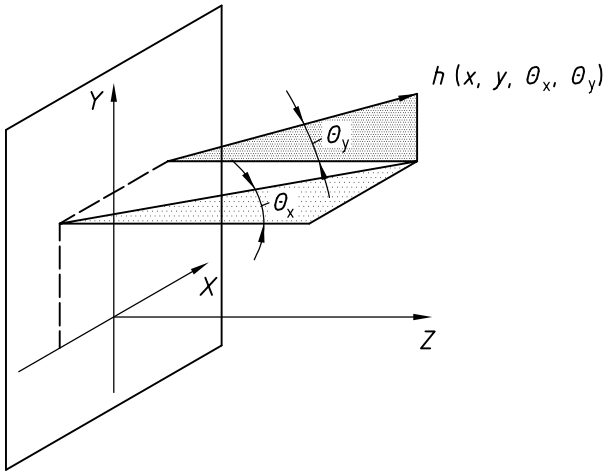

x,y spatial coordinates

Θ_x, Θ_y corresponding angular coordinates

Figure 1 — Coordinates of Wigner distribution

The power density distribution $E(x,y)$ in a measurement plane is related to the Wigner distribution by

$$E(x,y) = \int_{-\infty}^{\infty} h(x,y,\Theta_x,\Theta_y)\,\mathrm{d}\Theta_x\mathrm{d}\Theta_y \tag{1}$$

NOTE The integration limits in the equation above are finite, representing the maximum angles of the rays contained in the beam, in paraxial; they are conventionally extended to infinity.

2.3 First- and second-order moments of Wigner distribution

The first-order moments of the Wigner distribution are defined as

$$\langle x\rangle = \frac{1}{P}\int h(x,y,\Theta_x,\Theta_y)\,x\,\mathrm{d}x\mathrm{d}y\mathrm{d}\Theta_x\mathrm{d}\Theta_y \tag{2}$$

$$\langle y\rangle = \frac{1}{P}\int h(x,y,\Theta_x,\Theta_y)\,y\,\mathrm{d}x\mathrm{d}y\mathrm{d}\Theta_x\mathrm{d}\Theta_y \tag{3}$$

$$\langle \Theta_x\rangle = \frac{1}{P}\int h(x,y,\Theta_x,\Theta_y)\,\Theta_x\,\mathrm{d}x\mathrm{d}y\mathrm{d}\Theta_x\mathrm{d}\Theta_y \tag{4}$$

$$\langle \Theta_y\rangle = \frac{1}{P}\int h(x,y,\Theta_x,\Theta_y)\,\Theta_y\,\mathrm{d}x\mathrm{d}y\mathrm{d}\Theta_x\mathrm{d}\Theta_y \tag{5}$$

where P is the beam power given by

$$P = \int h(x,y,\Theta_x,\Theta_y)\,\mathrm{d}x\mathrm{d}y\mathrm{d}\Theta_x\mathrm{d}\Theta_y \tag{6}$$

or, using Equation (1),

$$P = \int E(x,y)\,\mathrm{d}x\mathrm{d}y \tag{7}$$

The spatial moments $\langle x \rangle$ and $\langle y \rangle$ give the lateral position of the beam centroid in the measurement plane. The angular moments $\langle \Theta_x \rangle$ and $\langle \Theta_y \rangle$ specify the direction of propagation of the beam centroid.

The (centred) second-order moments are given by

$$\left\langle x^k y^\ell \Theta_x^m \Theta_y^n \right\rangle = \frac{1}{P} \int_{-\infty}^{\infty} h\left(x, y, \Theta_x, \Theta_y\right) \left(x - \langle x \rangle\right)^k \left(y - \langle y \rangle\right)^\ell \left(\Theta_x - \langle \Theta_x \rangle\right)^m \left(\Theta_y - \langle \Theta_y \rangle\right)^n \mathrm{d}x\mathrm{d}y\mathrm{d}\Theta_x\mathrm{d}\Theta_y \tag{8}$$

where k, ℓ, m and n are non-negative integers and $k + \ell + m + n = 2$. Therefore, there are ten different second-order moments.

The three spatial second-order moments $\left\langle x^2 \right\rangle, \left\langle y^2 \right\rangle$ and $\langle x\, y \rangle$ are related to the lateral extent of the power density distribution in the measurement plane, the three angular moments $\left\langle \Theta_x^2 \right\rangle, \left\langle \Theta_y^2 \right\rangle$ and $\left\langle \Theta_x \Theta_y \right\rangle$ to the beam divergence, and the four mixed moments $\left\langle x\Theta_x \right\rangle, \left\langle x\Theta_y \right\rangle, \left\langle y\Theta_x \right\rangle$ and $\left\langle y\Theta_y \right\rangle$ to the phase properties in the measurement plane. More details on the relation between the ten second-order moments and the physical beam properties are discussed below.

The spatial first- and second-order moments can be directly obtained from the power density distribution $E(x,y)$. From Equation (1) it follows:

$$\langle x \rangle = \frac{1}{P} \int E\left(x, y\right) x \mathrm{d}x\mathrm{d}y \tag{9}$$

$$\langle y \rangle = \frac{1}{P} \int E\left(x, y\right) y \mathrm{d}x\mathrm{d}y \tag{10}$$

and

$$\left\langle x^2 \right\rangle = \frac{1}{P} \int E\left(x, y\right) \left(x - \langle x \rangle\right)^2 \mathrm{d}x\mathrm{d}y \tag{11}$$

$$\langle xy \rangle = \frac{1}{P} \int E\left(x, y\right) \left(x - \langle x \rangle\right) \left(y - \langle y \rangle\right) \mathrm{d}x\mathrm{d}y \tag{12}$$

$$\left\langle y^2 \right\rangle = \frac{1}{P} \int E\left(x, y\right) \left(y - \langle y \rangle\right)^2 \mathrm{d}x\mathrm{d}y \tag{13}$$

The other second-order moments are obtained by measuring the spatial moments in other planes and using the propagation law of the second-order moments (see below).

NOTE The details of measuring all ten second-order moments are given in ISO 11146-2.

2.4 Beam matrix

The ten second-order moments are collected into the symmetric 4 × 4 beam matrix

$$\boldsymbol{P} = \begin{pmatrix} \boldsymbol{W} & \boldsymbol{M} \\ \boldsymbol{M}^{\mathsf{T}} & \boldsymbol{U} \end{pmatrix} = \begin{pmatrix} \langle x^2 \rangle & \langle xy \rangle & \langle x\Theta_x \rangle & \langle x\Theta_y \rangle \\ \langle xy \rangle & \langle y^2 \rangle & \langle y\Theta_x \rangle & \langle y\Theta_y \rangle \\ \langle x\Theta_x \rangle & \langle y\Theta_x \rangle & \langle \Theta_x^2 \rangle & \langle \Theta_x\Theta_y \rangle \\ \langle x\Theta_y \rangle & \langle y\Theta_y \rangle & \langle \Theta_x\Theta_y \rangle & \langle \Theta_x^2 \rangle \end{pmatrix} \tag{14}$$

with the symmetric submatrix of the spatial moments

$$\boldsymbol{W} = \begin{pmatrix} \langle x^2 \rangle & \langle xy \rangle \\ \langle xy \rangle & \langle y^2 \rangle \end{pmatrix} \tag{15}$$

the symmetric submatrix of the angular moments

$$\boldsymbol{U} = \begin{pmatrix} \langle \Theta_x^2 \rangle & \langle \Theta_y\Theta_y \rangle \\ \langle \Theta_y\Theta_y \rangle & \langle \Theta_y^2 \rangle \end{pmatrix} \tag{16}$$

and the submatrix of the mixed moments

$$\boldsymbol{M} = \begin{pmatrix} \langle x\Theta_x \rangle & \langle x\Theta_y \rangle \\ \langle y\Theta_x \rangle & \langle y\Theta_y \rangle \end{pmatrix} \tag{17}$$

2.5 Propagation though aberration-free optical systems

Aberration-free optical systems are represented by 4×4 system matrices $\boldsymbol{S}$ known from geometrical optics. The propagation of the second-order moments through such a system is given by

$$\boldsymbol{P}_{\text{out}} = \boldsymbol{S} \cdot \boldsymbol{P}_{\text{in}} \cdot \boldsymbol{S}^{\mathsf{T}} \tag{18}$$

where $\boldsymbol{P}_{\text{in}}$ and $\boldsymbol{P}_{\text{out}}$ are the beam matrices in entry and exit plane of the optical system, respectively.

Examples for system matrices are given in Annex A.

2.6 Relation between second-order moments and physical beam quantities

The ten second-order moments are closely related to well known physical quantities of a beam.

The three spatial moments describe the lateral extent of the power density distribution of the beam in the measurement plane. The directions of minimum and maximum extent, called principal axes, are always orthogonal to each other. Any power density distribution is characterized by the extents along its principal axes and the orientation of those axes. The beam width along the direction of the principal axis that is closer to the x-axis of the laboratory system is given by

$$d_{\sigma x} = 2\sqrt{2}\left\{\left(\langle x^2 \rangle + \langle y^2 \rangle\right) + \gamma\left[\left(\langle x^2 \rangle - \langle y^2 \rangle\right)^2 + 4\left(\langle xy \rangle\right)^2\right]^{\frac{1}{2}}\right\}^{\frac{1}{2}} \tag{19}$$

and the beam width along the direction of that principal axis, which is closer to the y-axis by

$$d_{\sigma y} = 2\sqrt{2}\left\{\left(\left\langle x^2\right\rangle + \left\langle y^2\right\rangle\right) - \gamma\left[\left(\left\langle x^2\right\rangle - \left\langle y^2\right\rangle\right)^2 + 4\left(\left\langle x\,y\right\rangle\right)^2\right]^{\frac{1}{2}}\right\}^{\frac{1}{2}} \tag{20}$$

where

$$\gamma = \operatorname{sgn}\left(\left\langle x^2\right\rangle - \left\langle y^2\right\rangle\right) = \frac{\left\langle x^2\right\rangle - \left\langle y^2\right\rangle}{\left|\left\langle x^2\right\rangle - \left\langle y^2\right\rangle\right|} \tag{21}$$

If the principal axes make the angle + or − π/4 with x- or y-axis, when $\langle x^2\rangle = \langle y^2\rangle$, then $d_{\sigma x}$ is by convention the larger of the two beam widths, and

$$d_{\sigma x} = 2\sqrt{2}\left\{\left(\left\langle x^2\right\rangle + \left\langle y^2\right\rangle\right) + 2\left|\langle xy\rangle\right|\right\}^{\frac{1}{2}} \tag{22}$$

$$d_{\sigma y} = 2\sqrt{2}\left\{\left(\left\langle x^2\right\rangle + \left\langle y^2\right\rangle\right) - 2\left|\langle xy\rangle\right|\right\}^{\frac{1}{2}} \tag{23}$$

The azimuthal angle between that principal axis, which is closer to the x-axis, and the x-axis is obtained by

$$\varphi = \frac{1}{2}\arctan\left(2\langle xy\rangle \Big/ \left(\left\langle x^2\right\rangle - \left\langle y^2\right\rangle\right)\right) \tag{24}$$

valid for $\left\langle x^2\right\rangle \neq \left\langle y^2\right\rangle$; for $\left\langle x^2\right\rangle = \left\langle y^2\right\rangle$, $\varphi(z)$ is obtained as

$$\varphi(z) = \operatorname{sgn}\left(\langle xy\rangle\right)\cdot\frac{\pi}{4} \tag{25}$$

where

$$\operatorname{sgn}\left(\langle xy\rangle\right) = \frac{\langle xy\rangle}{\left|\langle xy\rangle\right|} \tag{26}$$

See Figure 2.

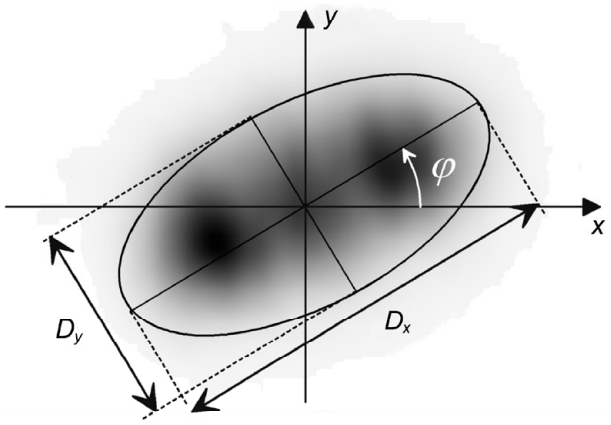

Figure 2 — Azimuthal angle and beam widths along principal axes of power density distribution

Very similar, the three angular moments describe the beam divergence characterized by the orthogonal directions of its maximum and minimum extent. These directions are called the principal axes of the beam divergence and may not coincide with the principal axes of the power density distribution in the measurement plane. The beam divergence along the direction of that principal axis, which is closer to the x-axis of the laboratory system is given by

$$\Theta_{\sigma x} = 2\sqrt{2}\left\{\left(\left\langle\Theta_x^2\right\rangle + \left\langle\Theta_y^2\right\rangle\right) + \tau\left[\left(\left\langle\Theta_x^2\right\rangle - \left\langle\Theta_y^2\right\rangle\right)^2 + 4\left(\left\langle\Theta_x\Theta_y\right\rangle\right)^2\right]^{\frac{1}{2}}\right\}^{\frac{1}{2}} \tag{27}$$

and the beam divergence along the direction of that principal axis, which is closer to the y-axis by

$$\Theta_{\sigma y} = 2\sqrt{2}\left\{\left(\left\langle\Theta_x^2\right\rangle + \left\langle\Theta_y^2\right\rangle\right) - \tau\left[\left(\left\langle\Theta_x^2\right\rangle - \left\langle\Theta_y^2\right\rangle\right)^2 + 4\left(\left\langle\Theta_x\Theta_y\right\rangle\right)^2\right]^{\frac{1}{2}}\right\}^{\frac{1}{2}} \tag{28}$$

where

$$\tau = \operatorname{sgn}\left(\left\langle\Theta_x^2\right\rangle - \left\langle\Theta_y^2\right\rangle\right) = \frac{\left\langle\Theta_x^2\right\rangle - \left\langle\Theta_y^2\right\rangle}{\left|\left\langle\Theta_x^2\right\rangle - \left\langle\Theta_y^2\right\rangle\right|} \tag{29}$$

If the principal axes of the beam divergence make the angle $+$ or $-\pi/4$ with x- or y-axis, when $\langle\Theta_x\rangle = \langle\Theta_y\rangle$, then $\Theta_{\sigma x}$ is by convention the larger of the two beam divergences, and

$$\Theta_{\sigma x} = 2\sqrt{2}\left\{\left(\left\langle\Theta_x^2\right\rangle + \left\langle\Theta_y^2\right\rangle\right) + 2\left|\left\langle\Theta_x\Theta_y\right\rangle\right|\right\}^{\frac{1}{2}} \tag{30}$$

$$\Theta_{\sigma y} = 2\sqrt{2}\left\{\left(\left\langle\Theta_x^2\right\rangle + \left\langle\Theta_y^2\right\rangle\right) - 2\left|\left\langle\Theta_x\Theta_y\right\rangle\right|\right\}^{\frac{1}{2}} \tag{31}$$

The divergence azimuthal angle between that principal axis, which is closer to the x-axis, and the x-axis is obtained by

$$\varphi_\Theta = \frac{1}{2}\arctan\left(2\left\langle\Theta_x\Theta_y\right\rangle \Big/ \left(\left\langle\Theta_x^2\right\rangle - \left\langle\Theta_y^2\right\rangle\right)\right) \tag{32}$$

valid for $\left\langle\Theta_x^2\right\rangle \neq \left\langle\Theta_y^2\right\rangle$; for $\left\langle\Theta_x^2\right\rangle = \left\langle\Theta_y^2\right\rangle$, $\varphi_\Theta(z)$ is obtained as

$$\varphi_\Theta(z) = \operatorname{sgn}\left(\left\langle\Theta_x\Theta_y\right\rangle\right)\cdot\frac{\pi}{4} \tag{33}$$

where

$$\operatorname{sgn}\left(\left\langle\Theta_x\Theta_y\right\rangle\right) = \frac{\left\langle\Theta_x\Theta_y\right\rangle}{\left|\left\langle\Theta_x\Theta_y\right\rangle\right|} \tag{34}$$

The four mixed moments are related to the average phase properties of the beam in the measurement plane. The best-fitting phase paraboloid is characterized by the orthogonal directions of maximum and minimum curvature. These curvatures can take also negative or zero values, independently, along the principal axes. The directions of maximum and minimum curvature, called the principal axes of the phase paraboloid, may

not coincide with the principal axes of the power density distribution in the measurement plane nor with the principal axes of the beam divergence. To retrieve the azimuthal angle of the these principal axes and the radii of curvature of the average phase front along them, the curvature matrix $\boldsymbol{C}$ has to be calculated by

$$\boldsymbol{C} = \begin{pmatrix} C_{xx} & C_{xy} \\ C_{xy} & C_{yy} \end{pmatrix} = \left(\boldsymbol{A} - \boldsymbol{A}^T \right)^{-1} \cdot \left(\boldsymbol{B} - \boldsymbol{B}^T \right) \cdot \boldsymbol{A} - \boldsymbol{B} \tag{35}$$

where

$$\boldsymbol{A} = \begin{pmatrix} 0 & 1 \\ -1 & 0 \end{pmatrix} \cdot \boldsymbol{W}^{-1} \tag{36}$$

and

$$\boldsymbol{B} = \boldsymbol{M} \cdot \boldsymbol{W}^{-1} \tag{37}$$

The radius of curvature of the average phase front along the direction of that principal axis, which is closer to the x-axis of the laboratory system, is given by

$$R_x = -\frac{2}{\left(C_{xx} + C_{yy} \right) + \mu \sqrt{\left(C_{xx} - C_{yy} \right)^2 + 4C_{xy}^2}} \tag{38}$$

and, similarly, the radius of curvature of the average phase front along the direction of that principal axis, which is closer to the y-axis by

$$R_y = -\frac{2}{\left(C_{xx} + C_{yy} \right) - \mu \sqrt{\left(C_{xx} - C_{yy} \right)^2 + 4C_{xy}^2}} \tag{39}$$

where

$$\mu = \operatorname{sgn}\left(C_{xx} - C_{yy} \right) = \frac{C_{xx} - C_{yy}}{\left| C_{xx} - C_{yy} \right|} \tag{40}$$

If the principal axes of the average phase curvature make the angle $+$ or $-\pi/4$ with the x- or y-axis, i.e. when $C_{xx} = C_{yy}$, then R_x is by convention the larger of the two principal radii (including the sign), and

$$R_x = -\frac{2}{\left(C_{xx} + C_{yy} \right) + 2\left| C_{xy} \right|} \tag{41}$$

$$R_y = -\frac{2}{\left(C_{xx} + C_{yy} \right) - 2\left| C_{xy} \right|} \tag{42}$$

The phase curvature azimuthal angle between that principal axis, which is closer to the x-axis, and the x-axis is obtained by

$$\varphi_P = \frac{1}{2} \arctan\left[2C_{xy} \Big/ \left(C_{xx} - C_{yy} \right) \right] \tag{43}$$

valid for $C_{xx} \neq C_{yy}$; for $C_{xx} = C_{yy}$ the phase curvature azimuthal angle is obtained by

$$\varphi_P = \mathrm{sgn}\left(C_{xy}\right) \cdot \frac{\pi}{4} \tag{44}$$

where

$$\mathrm{sgn}\left(C_{xy}\right) = \frac{C_{xy}}{\left|C_{xy}\right|} \tag{45}$$

Another physical beam parameter related to the phase properties is the twist parameter t defined as

$$t = \left\langle x\Theta_y \right\rangle - \left\langle y\Theta_x \right\rangle$$

The twist parameter is proportional to the orbital angular momentum of the beam and is invariant under propagation through stigmatic optical systems.

2.7 Propagation invariants

From the propagation law of the beam matrix the invariance of the following two independent quantities results.

The effective beam propagation ratio is defined as

$$M_{\mathrm{eff}}^2 = \frac{4\pi}{\lambda}\left[\det\left(\boldsymbol{P}\right)\right]^{\frac{1}{4}} \geqslant 1 \tag{46}$$

and the intrinsic astigmatism as

$$a = \frac{8\pi^2}{\lambda^2}\left(\left(\left\langle x^2\right\rangle\left\langle \Theta_x^2\right\rangle - \left\langle x\Theta_x\right\rangle^2\right) + \left(\left\langle y^2\right\rangle\left\langle \Theta_y^2\right\rangle - \left\langle y\Theta_y\right\rangle^2\right) + 2\left(\left\langle xy\right\rangle\left\langle \Theta_x\Theta_y\right\rangle - \left\langle x\Theta_y\right\rangle\left\langle y\Theta_x\right\rangle\right)\right) - (M_{\mathrm{eff}}^2)^2 \geqslant 0 \tag{47}$$

The effective beam propagation ratio is related to the focusability of a beam.

NOTE More general beam propagation ratio is a measure for the overall beam spread, or overall near- and far-field localization.

For a stigmatic beam (see below) the effective beam propagation ratio equals the beam propagation ratio:

$$M_{\mathrm{eff}}^2 = M^2 \tag{48}$$

For simple astigmatic beams (see below) having $M_x^2 \neq M_y^2$, the effective beam propagation ratio equals the geometric mean of the beam propagation ratios along both principal axes of the beam:

$$M_{\mathrm{eff}}^2 = \sqrt{M_x^2 M_y^2} \tag{49}$$

The intrinsic astigmatism is related to the visible and hidden astigmatism of a beam. For a stigmatic beam the intrinsic astigmatism a vanishes. For a simple astigmatic beam the intrinsic astigmatism a is given by

$$a = \frac{1}{2}\left(M_x^2 - M_y^2\right)^2 \tag{50}$$

These quantities are invariant under propagation in lossless and aberration-free optical systems only. In other systems they may vary. Any combinations of these invariants are also invariant.

2.8 Geometrical classification

Beams may be classified according to their propagation behaviour in stigmatic or simple astigmatic optical systems. A stigmatic system is an optical system that can be realized using ideal spherical lenses only. A simple astigmatic system is an optical system that can be realized using ideal cylindrical lenses all having the same orientation.

Geometrical beam classification refers to the symmetry of the power density distributions a beam takes on under propagation. The term “symmetry” is meant in the sense of the second-order moments. A power density distribution is classified as circular if the ratio of the minimum beam width to the maximum beam width, both measured along the principal axes, is greater than 0,87. Otherwise it is classified as elliptical.

NOTE In this sense even flat top power density distribution with a square shaped footprint is classified as circular.

Elliptical power density distributions are characterized by their orientation, specified by the azimuthal angle φ. Under free space propagation the power density distributions of a beam may all be circular, all be elliptical or some may be circular and some elliptical.

A beam is called stigmatic if all power density distributions under free propagation are circular and, in addition, if the beam were to pass through a cylindrical lens of arbitrary orientation, all of the elliptical power density distributions behind the lens have the same or orthogonal orientation as the axis parallel to the cylindrical surface of the lens.

A beam is called simple astigmatic if all elliptical power density distributions have the same (or orthogonal) azimuthal orientation under free space propagation and, in addition, were the beam to pass through a cylindrical lens of the same orientation as the beam, all of the elliptical power density distributions behind the lens would have the same or orthogonal orientation as the cylindrical lens.

All other beams are classified as general astigmatic.

Geometrical beam classification can be derived from the beam matrix. If all three submatrices $\boldsymbol{W}$, $\boldsymbol{M}$, and $\boldsymbol{U}$ are approximately proportional to the identity matrix, the beam is stigmatic. A beam is simple astigmatic and aligned with the axes x and y if all its submatrices $\boldsymbol{W}$, $\boldsymbol{M}$, and $\boldsymbol{U}$ are diagonal. A beam is simple astigmatic, but rotated with an azimuthal angle φ, if the submatrix $\boldsymbol{M}$ is approximately symmetric, i.e. the twist parameter t vanishes, and the principal axes of the power density distribution in the measurement plane, the principal axes of the beam divergences and those of the phase paraboloid approximately do coincide:

$$\varphi \approx \varphi_{\Theta} \approx \varphi_{\mathrm{P}} \tag{51}$$

All other beams are geometrically classified as general astigmatic.

2.9 Intrinsic classification

The geometrical classification of a beam may change after passing an optical system. But it can be shown that not any beam can be transformed into a stigmatic one. The possibility of a beam being transformed into a stigmatic beam is called *intrinsic stigmatism*. Hence, a simple astigmatic or even general astigmatic beam may be classified as intrinsic stigmatic.

A beam is classified as intrinsic stigmatic if

$$\frac{a}{\left(M^2_{\mathrm{eff}}\right)^2} < 0{,}039 \tag{52}$$

NOTE The threshold of 0,039 is in coincidence with the threshold value of 0,87 for the circularity of power density distributions. It ensures that a geometrically stigmatic beam is also intrinsic stigmatic.

3 Background and offset correction

3.1 General

Signals recorded as the measured power density distribution $E_{meas}(x,y)$ or $H_{meas}(x,y)$ can be divided into two parts: the "true" power density distribution $E(x,y)$ or $H(x,y)$, generated by the beam under test, and a possibly inhomogeneous background map $E_B(x,y)$, generated by other sources such as external or ambient radiation or by the sensor device itself (noise):

$$E_{meas}(x,y) = E(x,y) + E_B(x,y) \tag{53}$$

where the background signals can be further divided into a homogeneous part $E_{B,offset}$ (Baseline offset), an inhomogeneous part $E_{B,inh}(x,y)$ (for example baseline tilt) and the high-frequency noise components $E_{B,noise}(x,y)$.

$$E_B(x,y) = E_{B,offset}(x,y) + E_{B,inh}(x,y) + E_{B,noise}(x,y) \tag{54}$$

NOTE Usually, neither can the high-frequency noise components be corrected nor is it necessary to do so. Due to the integrations involved in calculating beam parameters the high-frequency noise components determine the intrinsic statistical errors and therefore affect only the reproducibility of the measurements, whereas the other background signals cause systematic errors.

The background distribution can be characterized by its mean value ($E_{B,offset}$) and its standard deviation ($E_{B,\sigma}$). If the variations of the background signal across the detector, which can be characterized by the differences of local mean values to the overall mean value, are smaller than the standard deviation $E_{B,\sigma}$ the detector background can be considered as homogeneous (cf. 3.4).

Before evaluating the beam parameters, background correction procedures have to be applied to prevent background signals in the wings of the distribution from dominating the integrals involved. In a first step a coarse correction has to be carried out by subtracting either a background map or an average background from the measured power density distribution. For detection systems having a constant background level across the full area of the sensor, average background level subtraction correction can be used. In all other cases the subtraction of the complete background map is necessary.

The subtraction of a background map or an average background determined from a background map (see 3.2 and 3.3) may provide offset errors of less than 0,1 digits in most cases, but do not always result in a baseline offset of zero. Due to the statistical nature of the background noise (the baseline offset is defined as the average of all non-illuminated pixels), to fluctuations of ambient radiation sources, or to scattered light or other non-coherent light emissions caused by the laser (for example fluorescence and/or residual pump light), the baseline offset can only be determined exactly from the measured power density distribution. Even small baseline offsets can create large errors in the evaluation of parameters characterizing the measured power density distribution. Therefore, especially for small beams (beam widths of less than 0,25 times the detector dimensions), the additional procedures given in 3.4 have to be applied.

As a result of a proper background subtraction there must exist negative noise values in the corrected power density distribution. These negative values have to be included in the further evaluation in order to allow compensation of positive noise amplitudes.

3.2 Coarse correction by background map subtraction

Using the identical experimental arrangement, the recording of a "dark image" background map has to be made immediately prior to the acquisition of a power density distribution "signal map". For cw-lasers the beam must be blocked at the position, where the beam exits the laser enclosure; for pulsed lasers data acquisition can be performed without triggering the laser.

An average detector background map is derived by recording and averaging at least $n > 10$ individual measurements of the background distribution:

$$\overline{E_{\mathrm{B}}(x,y)} = \frac{1}{n}\sum_{i=1}^{n} E_{\mathrm{B}}(x,y)_i \tag{55}$$

Using background map subtraction, the corrected distribution is then given by:

$$E(x,y) = E_{\mathrm{meas}}(x,y) - \overline{E_{\mathrm{B}}(x,y)} \tag{56}$$

In cases where temporally fluctuating residual ambient radiation is incident on the detector, which could distort the results, measurements of background and signal map should be performed in direct succession. For pulsed lasers or cw-lasers with a fast shutter, this can be achieved using consecutive acquisition cycles of the detector system in combination with "on-line" subtraction of the background. Furthermore, the provisions of 3.4 apply.

Subtracting a background map does not always result in a baseline offset of zero. Even small baseline offsets can create large errors in the evaluation of parameters characterizing the measured power density distribution. Care must be taken to minimize these baseline offset errors (see 3.4).

3.3 Coarse correction by average background subtraction

For detection systems having a constant background level across the complete area of the sensor, correction of measured distributions by average background level subtraction can be used.

An average detector background level $E_{\mathrm{B,offset}}$ across the area of the sensor is derived by recording and averaging across the detector at least $n > 10$ individual measurements of the background distribution:

$$\overline{E_{\mathrm{B,offset}}} = \frac{1}{m \cdot n}\sum_{i=1}^{n}\sum_{x,y=1}^{m} E_{\mathrm{B}}(x,y)_i \tag{57}$$

where m is the total number of individual (x,y) data recording points on the detector.

Using average background subtraction, the corrected distribution is given by

$$E(x,y) = E_{\mathrm{meas}}(x,y) - \overline{E_B(x,y)} \tag{58}$$

Subtracting an average background determined from a background map does not always result in a baseline offset of zero. Even small baseline offsets can create large errors in the evaluation of parameters characterizing the measured power density distribution. Care must be taken to minimize these baseline offset errors (see 3.4).

The procedures given in 3.2 and 3.3 could provide in most cases offset errors less than 0,1 digits. Especially for small beams (beam widths less than 0,25 times the detector dimensions) the additional procedures given in 3.4 have to be applied.

3.4 Fine correction of baseline offset

3.4.1 General

The subtraction of a background map or an average background determined from a background map does not always result in a baseline offset of zero, due to the statistical nature of the background noise (the baseline offset is defined as the average of all non-illuminated pixels), to fluctuations of ambient radiation sources, or to scattered light or other non-coherent light emissions caused by the laser (e.g. fluorescence and/or residual pump light).

Therefore, the baseline offset can only be determined exactly from the measured power density distribution. All procedures which may give a measure for the baseline offset can be used. In the past, several procedures for this have been shown to be useful:

a) Fourier transform methods;

b) histogram methods;

c) statistical methods;

d) approximation methods.

Due to their mathematical simplicity, only the two latter methods will be discussed in the following.

3.4.2 Statistical method

The background distribution can be characterized by its mean value ($E_{\mathrm{B,offset}}$) and its standard deviation ($E_{\mathrm{B},\sigma}$). Guess-values for the baseline offset $E_{\mathrm{B,offset}}$ and the noise $E_{\mathrm{B},\sigma}$, may be either extracted from a non-illuminated dark image or from non-illuminated areas within the measured distribution (see 3.4.3). All pixels whose grey values $E_{i,j}$ exceed

$$E_{i,j} > E_{\mathrm{B,offset}} + n_{\mathrm{T}} E_{\mathrm{B},\sigma} \tag{59}$$

with $2 < n_{\mathrm{T}} < 4$ assumed to be illuminated and which must be included in beam width calculations. The other pixels are assumed to be non-illuminated, their average gives the baseline offset value, which has to be subtracted from the measured data. Since the measured power density distribution is always digitized, this procedure cannot be applied directly to the measured data. Therefore, a 2d-convolution (averaging sub-arrays of $n \times m$ pixels) of the measured image has to be calculated:

$$\tilde{E}_{i,j} = \frac{1}{(m+1)\cdot(n+1)} \sum_{r=i-\frac{n}{2}}^{r=i+\frac{n}{2}} \sum_{s=j-\frac{m}{2}}^{s=j+\frac{m}{2}} E_{r,s} \tag{60}$$

and the following condition has to be applied to determine the illuminated pixels:

$$E_{i,j} > E_{\mathrm{B,offset}} + n_T \frac{\tilde{E}_{B,\sigma}}{\sqrt{(n+1)(m+1)}} \tag{61}$$

with $2 < n_{\mathrm{T}} < 4$.

The baseline offset, which has to be subtracted from the measured image, is then given by the mean value of the non-illuminated pixels. Practical values for m and n are between 2 % and 5 % of the image size. The convolution image is only used for the determination of non-illuminated pixels, the subsequent evaluation has to be applied to the offset corrected measured image.

NOTE This procedure is basically related to thresholding the image. In contrast to conventional thresholding methods, where the threshold value can only be set to full digits, using this method no additional measurement errors are introduced and no information is lost.

3.4.3 Approximation method

This method may not only provide guess-values for the statistical method. In many cases the accuracy of this offset fine correction will be sufficient.

NOTE The power density distribution of a non-diffracted laser beam rapidly falls off with increasing distance to its centre. Therefore, when the beam width does not exceed 0,5 times the detector size there usually exist areas within the measured distribution which are not illuminated by the laser beam, most probably the corners of the image.

Determining the baseline offset by averaging a sample of N non-illuminated points (for example arrays of $n \times m$ pixels in each of the four corners) within the image directly gives the offset, which has to be subtracted from the measured distribution. The uncertainty of the offset is then related.

EXAMPLE Using a standard CCD camera with a noise of 1 digit and $n = m = 50$, the remaining offset uncertainty is 1/100 digits.

Practical values for m and n are between 2 % and 5 % of the image size.

The validity of this method should be checked by comparing the baseline offset of the measured distribution to those obtained for a dark image, where the same areas are used for averaging:

$$\frac{\left|E_{\text{offset,meas}} - E_{\text{offset,dark}}\right|\sqrt{N}}{E_{\text{B},\sigma}} < n_t \tag{62}$$

where n_t should be less than four.

If the above relation does not hold, this indicates that there is either a significant amount of additional radiation that does not occur with the beam blocked, or that the beam size is too large compared to the detector size, so that the corners are illuminated. In this case one of the following procedures have to be chosen:

a) use of beam-forming optics with lower total integrated scatter;

b) re-imaging of the beam with lower magnification or choosing a larger detector size;

c) improved shielding against ambient radiation and non-coherent resonator light.

4 Alternative methods for beam width measurements

4.1 General

If measurement equipment with a sufficiently high signal-to-noise ratio and a simultaneously high spatial resolution is not available, alternative methods, described in this section, may be used. These methods allow measurement of beam width or beam diameter, with an accuracy which is acceptable in many cases, using rather simple equipment.

The evaluation methods described in this section are not based on the determination of the second-order moments of the spatial power distribution function, necessary for obtaining a consistent propagation formalism.

The relation between the second-order moment diameter and the diameter based on the alternative definition strongly depends on the shape of the power density distribution[4].

However, it has been demonstrated that at least for several cases (see Table 1) there exists a correlation between the beam propagation ratios determined using one of the alternative methods, and the results of the standard method described in this part of ISO 11146.

This can be written as

$$\sqrt{M^2} = c_i(\sqrt{M_i^2} - 1) + 1 \tag{63}$$

where

M_i^2 is the beam propagation ratio according to alternative method i;

c_i is the correlation factor between alternative method i and the standard method.

Table 1 — Alternative methods — Connection factors

Alternative method	c_i
Variable aperture (see 4.2)	1,14
Moving knife-edge (see 4.3)	0,81
Moving slit (see 4.4)	0,95
NOTE These c_i were verified for gas laser beams with stable resonator geometries and power up to 10 W (and for CO_2 laser beams up to 1 kW) and with M^2 up to $M^2 = 4$, for stigmatic beams. For higher M^2 values and other types of lasers, the correlation factors need to be verified.	

From this relationship between the beam propagation ratios, an M^2-dependent correlation factor can be derived for the determination of the beam diameters (widths):

$$d_\sigma = \frac{d_i}{M_i}\left[c_i\left(\sqrt{M_i^2} - 1\right) + 1\right] \tag{64}$$

where d_i is the beam diameter or beam width according to alternative method i.

Each of the three alternative methods is described below.

4.2 Variable aperture method

4.2.1 Test principle

A variable diaphragm located at the plane of measurement is used to determine the fraction of transmitted power as a function of the diameter of the aperture (see Figure 3). The uncorrected diameter of the beam is defined by the minimum aperture diameter which allows transmission of 86,5 % of the total beam power. The beam diameter can be calculated using the equation given in 4.2.5.

This method can only be used for beams with a ratio of principal axes not exceeding 1,15:1.

4.2.2 Detector

The radiation detector should be in accordance with IEC 61040:1990, in particular, Clauses 3 and 4 of that International Standard. Furthermore, the following points should be noted.

— It has to be confirmed, from manufacturers' data or by measurement, that the output quantity of the detector system (e.g. the voltage) is linearly dependent on the input quantity (laser power). Any wavelength dependency, non-linearity or non-uniformity of the detector or the electronic device must be minimized or corrected by use of a calibration procedure.

— Care must be taken to ascertain the damage thresholds (for irradiance, radiant exposure, power and energy) of the detector surface so that it is not exceeded by the laser beam.

— Sensitivity must be uniform across the detector surface, and the detector must be insensitive to beam position within the measurement clear aperture.

— The detector size must be chosen so that more than 99 % of the total laser power is captured by the detector.

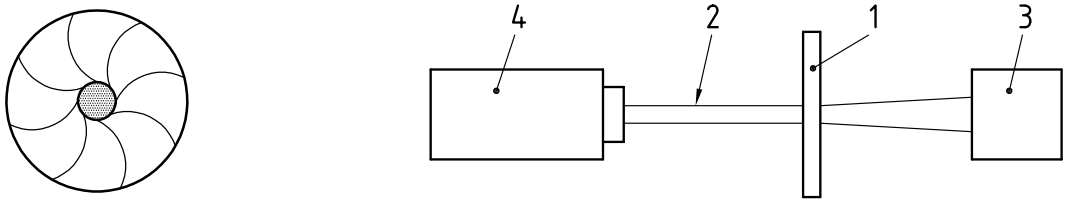

a) Axis (cut-away) view (detector side)

b) Top view

Key

1 variable diaphragm
2 beam
3 detector
4 laser

Figure 3 — Configuration for measuring variable-aperture beam width

4.2.3 Diaphragms/apertures

Select round diaphragms with diameters in steps such that the transmitted power is reduced by less than 5 % when changing from one size to the next.

Alternatively, it is permissible to use a variable diaphragm (iris) with calibrated aperture settings.

Diaphragms have to be constructed to maintain geometric shape during operation and absorption of the beam energy (may be water-cooled, reflective or use attenuation as specified in ISO 11146-1). For configuration, see Figure 3.

4.2.4 Test procedure

Assure that the aperture is perpendicular to the optical axis. Align the detector such that its measurement aperture is centred on the optical axis of the beam to an accuracy of at least 0,1 times the width to be measured. Centring procedure: Reduce aperture to approximately 80 % power transmission and move aperture to maximum power transmission.

Verify that the total beam power is incident on the detector surface, by introducing a diaphragm coaxial to the beam at the detector surface, such that it covers or occludes the outer 30 % of the detector area. No measurable change in detected power should occur.

Record total power (P_0).

Decrease aperture size in steps which cause a 5 % or less decrease in detected power. Record at least the aperture sizes the next greater (d_1) and the next smaller (d_2) than the aperture at the point at which power is reduced to 86,5 % of the original total power reading. At each of these size settings, record the respective power (P_1, P_2) or energy (Q_1, Q_2) readings.

4.2.5 Evaluation

Calculate the uncorrected beam diameter $d_{86,5}$ by linear interpolation between the known size apertures at the corresponding power level points above and below 86,5 % total power.

$$d_{86,5} = d_1 + \left[\left(P_{86,5} - P_1 \right) \cdot \left(d_2 - d_1 \right) / \left(P_2 - P_1 \right) \right] \tag{65}$$

Calculate the corresponding d_σ by using the equation

$$d_\sigma = d_{86,5} \frac{1}{\sqrt{M_{86,5}^2}} \left[1{,}14 \left(\sqrt{M_{86,5}^2 - 1} \right) + 1 \right] \tag{66}$$

For limitations, see 4.1.

4.3 Moving knife-edge method

4.3.1 Test principle

A moving knife-edge is used to cut the beam in front of a fixed large-area detector so that the detector measures the transmitted power as a function of the edge position (see Figure 4). The uncorrected beam width is given by twice the distance of the two knife-edge locations which are determined by 84 % and 16 % power transmission. The beam width can be calculated using Equations 67 and 68.

When dealing with elliptical beams, the moving direction of the knife-edge has to be chosen to coincide with the two principal beam axes.

4.3.2 Detector system

See 4.2.2. The requirements given in apply. The length of the knife-edge must be chosen such that it covers at least the diameter of the sensitive detector area.

4.3.3 Test procedure for stigmatic beams

Record the beam power with the knife-edge well out of the beam.

Move the translation stage until the x-axis knife-edge reduces the power transmitted to the power meter to 84 % of the initial power and record the position of the translation stage (x_1).

Continue moving the translation stage until only 16 % of the initial beam power is transmitted to the power meter and record the location of the translation stage (x_2).

4.3.4 Evaluation

Compute the uncorrected beam width d_k at this location according to

$$d_k = 2 \cdot (x_2 - x_1) \tag{67}$$

where $(x_2 - x_1)$ is the absolute value of the difference in translation stage position readings.

Calculate the corresponding d_σ according to

$$d_\sigma = d_k \cdot \frac{1}{\sqrt{M_k^2}} \left[0{,}81 \left(\sqrt{M_k^2 - 1} \right) + 1 \right] \tag{68}$$

For limitations, see 4.1.

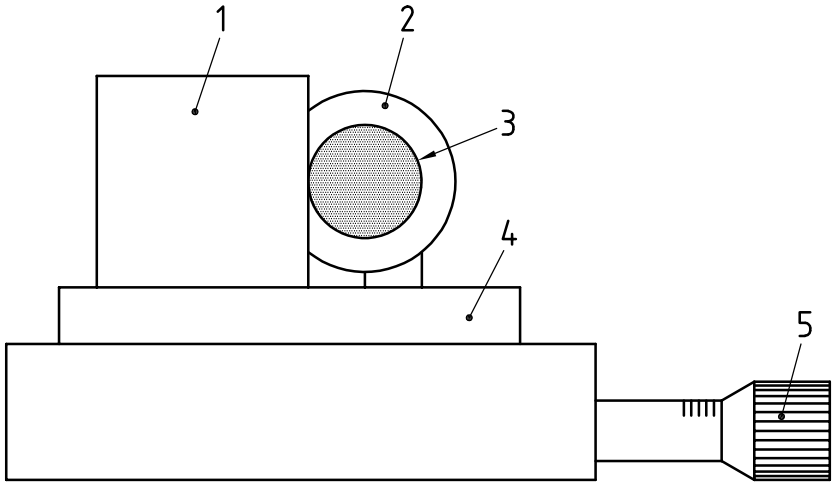

Key

1 knife-edge
2 photo cell collector
3 beam
4 translation stage
5 micrometer

Figure 4 — Configuration for measuring moving knife-edge beam width

4.3.5 Test procedure for simple astigmatic beams

Two measurements moving the knife-edge along the principal axes are necessary to obtain the beam widths $d_{\sigma x}$ and $d_{\sigma y}$ The procedure and evaluation are the same as those given in 4.3.3 and 4.3.4.

The principal axes can be determined as follows:

a) Determine two orthogonal moving directions for which the uncorrected beam widths are equal.

b) Rotate these two directions by 45° to yield the principal axes.

4.4 Moving slit method

4.4.1 Test principle

A slit mounted on a translation stage is used to cut the beam in front of a fixed large-area detector so that the detector measures the transmitted power as a function of the slit position (see Figure 5). The uncorrected beam width is given by the distance of the two slit positions where the power is 13,5 % of the maximum transmitted power. The beam width can be calculated using Equation 69.

When dealing with elliptical beams, the moving direction of the slit has to be chosen to coincide with the two principle beam axes.

NOTE By using a strip detector, and moving the slit and detector together, very consistent results can be obtained on larger diameter beams.

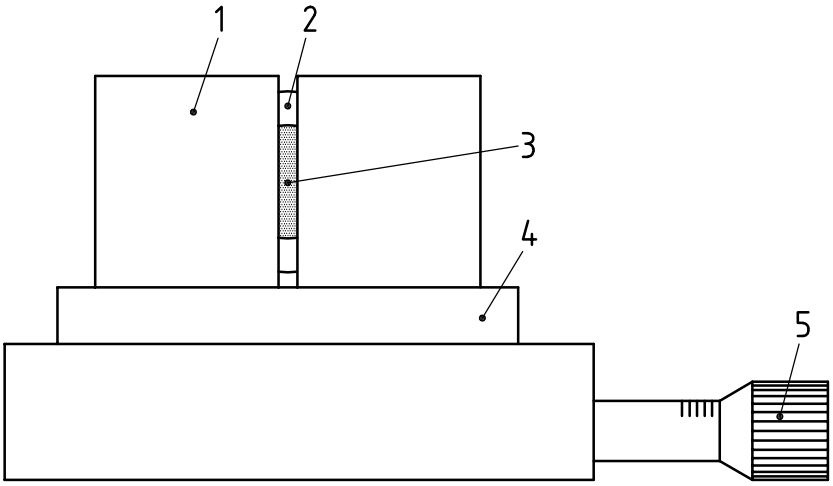

Key

1 moving slit
2 photo cell collector
3 beam
4 translation stage
5 micrometer

Figure 5 — Moving slit beam-width measuring setup

4.4.2 Detector system

See 4.2.2. The length of the slit must be chosen such that it covers at least the diameter of the sensitive detector area.

4.4.3 Slit

The slit length to be used must be not less than two times greater than the approximate beam width to be measured.

The slit width to be used has to be not more than 1/20 the approximated beam width to be measured.

4.4.4 Test procedure for stigmatic beams

Position the slit through (perpendicular to the propagation axis of) the beam such that maximum total power is transmitted through the opening to the detector. Record this as Reading 1.

Translate the slit laterally such that it allows only 13,5 % of the total (Reading 1) power to pass, at one edge of the beam. Record the position (x_1) of the slit.

Translate the slit laterally in the opposing direction, such that it allows only 13,5 % of the total transmitted power to pass at the opposing edge of the beam. Record the location (x_2) of the slit.

4.4.5 Evaluation

The distance between the positions ($x_2 - x_1$) is the uncorrected beam width d_S.

Calculate the corresponding d_σ by using the equation

$$d_\sigma = d_S \cdot \frac{1}{\sqrt{M_S^2}} \left[0{,}95 \left(\sqrt{M_S^2} - 1 \right) + 1 \right] \tag{69}$$

For limitations, see 4.1.

4.4.6 Test procedure for simple astigmatic beams

Two measurements moving the slit along the principal axes are necessary to obtain the beam widths $d_{\sigma x}$ and $d_{\sigma y}$. The procedure and evaluation are the same as given in 4.4.4 and 4.4.5.

The principal axes can be determined as follows.

a) Determine two orthogonal moving directions for which the uncorrected beam widths are equal.

b) Rotate these two directions by 45° to yield the principal axes.

Annex A
(informative)

Optical system matrices

Aberration-free optical systems are represented by 4×4 matrices. The propagation law given in 2.5 is based on these matrices and can easily be used to predict beam properties. In this annex the matrices for the most important optical elements are presented and the procedure for calculating the matrix of a combined optical system is given.

The matrix for free propagation over a distance of L is given by

$$\boldsymbol{S}_{\mathrm{P}}(L) = \begin{pmatrix} 1 & 0 & L & 0 \\ 0 & 1 & 0 & L \\ 0 & 0 & 1 & 0 \\ 0 & 0 & 0 & 1 \end{pmatrix} \tag{A.1}$$

A thin spherical lens of focal length f is represented by the matrix

$$\boldsymbol{S}_{\mathrm{SL}}(f) = \begin{pmatrix} 1 & 0 & 0 & 0 \\ 0 & 1 & 0 & 0 \\ -1/f & 0 & 1 & 0 \\ 0 & -1/f & 0 & 1 \end{pmatrix} \tag{A.2}$$

An aligned thin cylindrical lens is represented by the matrix

$$\boldsymbol{S}_{\mathrm{CL}}(f_x, f_y) = \begin{pmatrix} 1 & 0 & 0 & 0 \\ 0 & 1 & 0 & 0 \\ -1/f_x & 0 & 1 & 0 \\ 0 & -1/f_y & 0 & 1 \end{pmatrix} \tag{A.3}$$

where f_x and f_y are the focal lengths in the horizontal and vertical directions, respectively.

The matrix of a cylindrical lens rotated by an angle of α with respect to the horizontal axes is given by

$$\boldsymbol{S}_{\mathrm{RCL}}(f_x, f_y, \alpha) = \boldsymbol{R}(\alpha)^{\mathrm{T}} \cdot \boldsymbol{S}_{\mathrm{CL}}(f_x, f_y) \cdot \boldsymbol{R}(\alpha) \tag{A.4}$$

where

$$\boldsymbol{R}(\alpha) = \begin{pmatrix} \cos\alpha & \sin\alpha & 0 & 0 \\ -\sin\alpha & \cos\alpha & 0 & 0 \\ 0 & 0 & \cos\alpha & \sin\alpha \\ 0 & 0 & -\sin\alpha & \cos\alpha \end{pmatrix} \tag{A.5}$$

and $\boldsymbol{R}(\alpha)^{\mathrm{T}}$ is the transposed matrix of $\boldsymbol{R}(\alpha)$.

The matrix of an optical system of several optical elements combined is obtained by matrix multiplication. For example, the matrix consisting of a spherical lens of focal length f in a distance L_1 from the entry plane and a distance L_2 from the exit plane is given by

$$\boldsymbol{S} = \boldsymbol{S}_{\mathrm{P}}(L_2) \cdot \boldsymbol{S}_{\mathrm{SL}}(f) \cdot \boldsymbol{S}_{\mathrm{P}}(L_1) \tag{A.6}$$

Bibliography

[1] ISO 11146-1*, Lasers and laser-related equipment — Test methods for laser beam widths, divergence angles and beam propagation ratios — Part 1: Stigmatic and simple astigmatic beams* [1)]

[2] ISO 11146-2*, Lasers and laser-related equipment — Test methods for laser beam widths, divergence angles and beam propagation ratios — Part 2: General astigmatic beams* [1)]

[3] IEC 61040:1990*, Power and energy measuring detectors, instruments and equipment for laser radiation*

[4] SIEGMAN, A.E. *et al.,* "Choice of clip levels for beam width measurements using knife edge techniques", *IEEE Journal of Quantum Electronics* Vol. 27 p. 1098-1104 (1991)

[5] SIEGMAN, A.E., "Defining the effective radius of curvature for a nonideal optical beam", *IEEE Journal of Quantum Electronics* Vol. 27 p. 1146-1148 (1991)

[6] NEMES, G., "Synthesis of general astigmatic optical systems, the detwisting procedure, and the beam quality factors for general astigmatic laser beams", *Laser Beam Characterization*, H. Weber, N. Reng, J. Lüdtke, and P.M. Mejias, eds., Technical University Berlin, Institutes of Optics, Straße des 17. Juni 135, 10623 Berlin, Germany, p. 93-104 (1994)

[7] NEMES, G., *Intrinsic and geometrical beam classification and the beam identification after measurement,* SPIE Proc. 4932, p. 624-636 (2003)

1) To be published.

ICS 31.260

Price based on 22 pages